NOAA Technical Memorandum NESS 113

SATELLITE IDENTIFICATION OF SURFACE RADIANT TEMPERATURE FIELDS OF SUBPIXEL RESOLUTION

Washington, D.C.
December 1980

U.S. DEPARTMENT OF COMMERCE / National Oceanic and Atmospheric Administration / National Earth Satellite Service

NOAA TECHNICAL MEMORANDUMS

National Earth Satellite Service Series

The National Earth Satellite Service (NESS) is responsible for the establishment and operation of NOAA's environmental satellite systems.

NOAA Technical Memorandums facilitate rapid distribution of material that may be preliminary in nature and so may be published formally elsewhere at a later date. Publications 1 to 20 and 22 to 25 are in the earlier ESSA National Environmental Satellite Center Technical Memorandum (NESCTM) series. The current NOAA Technical Memorandum NESS series includes 21, 26, and subsequent issuances.

Publications listed below are available (also in microfiche form) from the National Technical Information Service, U.S. Department of Commerce, Sills Bldg., 5285 Port Royal Road, Springfield, VA 22161. Prices on request. Order by accession number (given in parentheses). Information on memorandums not listed below can be obtained from Environmental Data and Information Service (D822), 6009 Executive Boulevard, Rockville, MD 20852.

NESS 66 A Summary of the Radiometric Technology Model of the Ocean Surface in the Microwave Region. John C. Alishouse, March 1975, 24 pp. (COM-75-10849/AS)

NESS 67 Data Collection System Geostationary Operational Environmental Satellite: Preliminary Report. Merle L. Nelson, March 1975, 48 pp. (COM-75-10679/AS)

NESS 68 Atlantic Tropical Cyclone Classifications for 1974. Donald C. Gaby, Donald R. Cochran, James B. Lushine, Samuel C. Pearce, Arthur C. Pike, and Kenneth O. Poteat, April 1975, 6 pp. (COM-75-10676/AS)

NESS 69 Publications and Final Reports on Contracts and Grants, NESS-1974. April 1975, 7 pp. (COM-75-10850/AS)

NESS 70 Dependence of VTPR Transmittance Profiles and Observed Radiances on Spectral Line Shape Parameters. Charles Braun, July 1975, 17 pp. (COM-75-11234/AS)

NESS 71 Nimbus-5 Sounder Data Processing System, Part II: Results. W. L. Smith, H. M. Woolf, C. M. Hayden, and W. C. Shen, July 1975, 102 pp. (COM-75-11334/AS)

NESS 72 Radiation Budget Data From the Meteorological Satellites, ITOS 1 and NOAA 1. Donald H. Flanders and William L. Smith, August 1975, 20 pp. (PB-246-877/AS)

NESS 73 Operational Processing of Solar Proton Monitor Data (Revision of NOAA TM NESS 49). Stanley R. Brown, September 1975, 15 pp. (COM-73-11647)

NESS 74 Monthly Winter Snowline Variation in the Northern Hemisphere From Satellite Records, 1966-75. Donald R. Wiesnet and Michael Matson, November 1975, 21 pp. (PB-248-437/6ST)

NESS 75 Atlantic Tropical and Subtropical Cyclone Classifications for 1975. D. C. Gaby, J. B. Lushine, B. M. Mayfield, S. C. Pearce, and K.O. Poteat, March 1976, 14 pp. (PB-253-968/AS)

NESS 76 The Use of the Radiosonde in Deriving Temperature Soundings From the Nimbus and NOAA Satellite Data. Christopher M. Hayden, April 1976, 19 pp. (PB-256-755/AS)

NESS 77 Algorithm for Correcting the VHRR Imagery for Geometric Distortions Due to the Earth Curvature, Earth Rotation, and Spacecraft Roll Attitude Errors. Richard Legeckis and John Pritchard, April 1976, 31 pp. (PB-258-027/AS)

NESS 78 Satellite Derived Sea-Surface Temperatures From NOAA Spacecraft. Robert L. Brower, Hilda S. Gohrband, William G. Pichel, T. L. Signore, and Charles C. Walton, June 1976, 74 pp. (PB-258-026/AS)

NESS 79 Publications and Final Reports on Contracts and Grants, NESS-1975. National Environmental Satellite Service, June 1976, 10 pp. (PB-258-450/AS)

NESS 80 Satellite Images of Lake Erie Ice: January-March 1975. Michael C. McMillan and David Forsyth, June 1976, 15 pp. (PB-258-458/AS)

NESS 81 Estimation of Daily Precipitation Over China and the USSR Using Satellite Imagery. Walton A. Follansbee, September 1976, 30 pp. (PB-261-970/AS)

NESS 82 The GOES Data Collection System Platform Address Code. Wilfred E. Mazur, Jr., October 1976, 26 pp. (PB-261-968/AS)

NESS 83 River Basin Snow Mapping at the National Environmental Satellite Service. Stanley R. Schneider, Donald R. Wiesnet, and Michael C. McMillan, November, 1976, 19 pp. (PB-263-816/AS)

NESS 84 Winter Snow-Cover Maps of North America and Eurasia From Satellite Records, 1966-1976. Michael Matson, March 1977, 28 pp. (PB-267-393/AS)

NESS 85 A Relationship Between Weakening of Tropical Cyclone Cloud Patterns and Lessening of Wind Speed. James B. Lushine, March 1977, 12 pp. (PB-267-392/AS)

NESS 86 A Scheme for Estimating Convective Rainfall From Satellite Imagery. Roderick A. Scofield and Vincent J. Oliver, April 1977, 47 pp. (PB-270-762/AS)

(Continued on inside back cover)

NOAA Technical Memorandum NESS 113

SATELLITE IDENTIFICATION OF SURFACE RADIANT TEMPERATURE FIELDS OF SUBPIXEL RESOLUTION

Jeff Dozier

Washington, D.C.
December 1980

UNITED STATES
DEPARTMENT OF COMMERCE
Philip M. Klutznick, Secretary

NATIONAL OCEANIC AND
ATMOSPHERIC ADMINISTRATION
Richard A. Frank, Administrator

National Earth Satellite Service
David S. Johnson,
Assistant Administrator

Satellite Identification of Surface Radiant Temperature Fields of Subpixel Resolution

Jeff Dozier

NOAA National Earth Satellite Service
Earth Sciences Laboratory
Washington, DC 20233

(on leave from University of California, Santa Barbara)

ABSTRACT. A method is presented for identifying from NOAA TIROS-N series satellite data the magnitudes and subpixel areal coverages of two different surface radiant temperatures, using the different response of the Planck function at different wavelengths.

1. Introduction

Satellite spaceborne radiometers with more than one thermal infrared channel were originally designed to identify cloud-contaminated pixels and to evaluate the radiant contribution from atmospheric water vapor. However, over a surface with markedly varying temperatures at sub-pixel resolution, the different radiant temperatures sensed at different wavelengths may be more a result of the surface temperature field than of atmospheric interference with the signal.

Over a land surface with two different surface materials of different temperatures, the way in which the radiance contributions are averaged over a pixel will depend on the wavelength range of the sensor. If one part of a pixel is much warmer than the remainder, for example, that warm part will contribute proportionally more radiance to the signal in shorter wavelengths of the thermal infrared than in longer wavelengths. Through manipulation of the integral of the Planck function for the different channels, we can calculate (a) the radiant temperatures of one of two temperature fields of sub-pixel resolution; and (b) the portions of the pixel that each occupies. The portions of a pixel occupied by each temperature field are not necessarily contiguous, but the method assumes that there are only two temperature fields, with a "target" temperature and a "background" temperature.

2. TIROS-N Satellite Series Thermal Infrared Sensors

NOAA's TIROS-N series polar orbiting satellites now contain instrumentation for measuring upwelling thermal infrared radiation in more than one wavelength band. The Advanced Very High Resolution Radiometer (AVHRR) on NOAA-6 (launched June 1979), with a spatial resolution of 1.1 km, has two thermal infrared channels. On later satellites in the series, a third thermal channel will be added to the AVHRR. Wavelength ranges for these instruments are given in table 1.

Table 1
AVHRR Thermal Channels (from Schwalb 1979)

NOAA-6

channel	wavelength range (μm)
3	3.55 - 3.93
4	10.5 - 11.5

NOAA-7 and subsequent satellites

channel	wavelength range (μm)
3	3.53 - 3.93
4	10.4 - 11.3
5	11.4 - 12.4

Channels 3 and 4 on these satellites are in water vapor window regions of the electromagnetic spectrum. The design purpose of the two channels was to allow discrimination of cloud-contaminated pixels, and to provide a radiance measurement in a highly transmissive water vapor window, for the measurement of sea surface temperature, chiefly at night. The third thermal infrared channel will add capability to determine absolute sea surface temperature day or night.

3. Notation

c_1	first Planck constant ($3.741832\times10^{-16}\ W\,m^2$)
c_2	second Planck constant ($1.438786\times10^{-2}\ m\,K$)
$L(T)$	upwelling thermal radiance ($W\,m^{-2}\,sr^{-1}$) as a function of temperature
$L_j(T)$	integrated upwelling thermal radiance in channel j ($W\,m^{-2}\,sr^{-1}$)
p	portion of a pixel occupied by target
T	temperature (K)
T_j	radiant temperature measured by channel j (K)
T_b	background temperature (K)
T_t	target temperature (K)
$\beta(\lambda,T)$	Planck function ($W\,m^{-3}$)
ϵ	emissivity
λ	wavelength (μm or m)
$\Phi(\lambda)$	relative spectral response function of sensor (normalized to 1 at maximum value)

4. Radiance-Temperature Relations

In the absence of an atmospheric contribution or attenuation, the upwelling radiance sensed by a downward pointing radiometer is derived by integrating the product of Planck's function and the response function of the sensor:

$$L(T) = \frac{1}{\pi} \int_{\lambda_1}^{\lambda_2} \epsilon_\lambda\, \beta(\lambda,T)\, \Phi(\lambda)\, d\lambda \qquad (1)$$

For most Earth surfaces ϵ_λ is nearly independent of λ over the range of an AVHRR channel, so one can drop the λ subscript and move ϵ outside the integral in (1). The Planck function for the emittance at wavelength λ of a black body at temperature T is (Suits 1975)

$$\beta(\lambda,T) = \frac{c_1 \lambda^{-5}}{\exp\left(\dfrac{c_2}{\lambda T}\right) - 1}. \tag{2}$$

The spectral response function for the sensor $\Phi(\lambda)$ is zero outside the range $[\lambda_1, \lambda_2]$. For rough calculations it is often defined as a "gate function," i.e., equal to one within the range of values specified in table 1. Alternatively, it may be defined more precisely as a graphical or tabulated function, as figure 1 shows for channels 3 and 4 of NOAA-6.

Let us designate $L_3(T)$ and $L_4(T)$ to be the NOAA-6 channel 3 and 4 radiances as functions of blackbody temperature (i.e., $\epsilon = 1$), and the inverse functions by $L_3^{-1}()$ and $L_4^{-1}()$, respectively. For temperatures from 100 to 1000 K, eq. (1) was calculated numerically by an adaptive quadrature method (Forsythe *et al.* 1977, ch. 5). The resulting values for $L_3(T)$ and $L_4(T)$ are shown in figure 2. Here it is apparent that the shift in the peak of the Planck function toward shorter wavelengths, as temperature increases, causes the radiant contribution to channel 3 to increase more rapidly, at higher temperatures, than that to channel 4.

Now, suppose we have a "mixed pixel" composed of a target at temperature T_t which occupies portion p of the pixel (where $0 \leqslant p \leqslant 1$) and a background temperature T_b which occupies the remaining portion $(1-p)$ of the pixel. The radiant temperatures sensed by the AVHRR in channels 3 and 4 will be, in the absence of an atmospheric contribution or attenuation,

$$T_j = L_j^{-1}\left[p\, L_j(T_t) + (1-p)\, L_j(T_b)\right] \quad \Big\{ j=3,4\,. \tag{3}$$

For a reference background temperature $T_b = 285$, figure 3 shows values of T_3 and T_4 as functions of p for various values of T_t from 150 to 500 K. In figure 4 are plotted the differences $T_3 - T_4$ *vs.* p for the same situations.

5. Determination of T_t and p

Assume that we know the value of T_b, perhaps from measurements from surrounding pixels that contain no "target" surface. The two equations in (3) now have only two unknowns, p and T_t. From figure 3 it is evident that we can solve for them. For example, suppose $T_b = 285$, $T_3 = 325$, and $T_4 = 307$. The value of T_3 constrains the range of choices considerably, as shown by the dashed line in the lower graph in figure 3. The correct values for p (0.2) and T_t (371) can be selected from the value of T_4. Similarly, the correct value can be read from the difference $T_3 - T_4$ (18) in figure 4. Note that the largest differences between T_3 and T_4 occur when the pixel contains a small, hot target, or when a cold target covers almost all of the field of view. If the difference between T_t and T_b is not very large, the solution is insensitive to variations in p.

A mathematical solution that does not require the construction of graphs for every value of T_b is accomplished by rearranging eq. (3) in these simultaneous nonlinear equations:

$$L_j(T_j) - \left[p\, L_j(T_t) + (1-p)\, L_j(T_b)\right] = 0 \quad \Big\{ j=3,4\,. \tag{4}$$

Such sets of equations can be solved by several methods. I use a modification of Brent's (1973b) algorithm developed by Moré and Cosnard (1979). Convergence problems are reduced if Box's (1966) transformation is used to map the constrained temperatures into unconstrained variables.

6. Determination of T_t when T_b and p are Unknown

For some applications, for example determination of sea surface temperature, we have no reliable estimate of the background temperature T_b. However, suppose we assume that in two adjacent pixels the target (sea surface) temperatures T_t are the same and the background (cloud) temperatures T_b are the same, but that the cloud-covered portions $(1-p)$ are different.

Note that eq. (4) can be solved for p;

$$p = \frac{L_j(T_j) - L_j(T_b)}{L_j(T_t) - L_j(T_b)} \quad \Big\{ j=3,4 \,. \tag{5}$$

If we denote the non-cloud contaminated portions of two adjacent pixels as $p^{(1)}$ and $p^{(2)}$, and their radiant temperatures by $T_j^{(1)}$ and $T_j^{(2)}$, we can form the ratio

$$\frac{p^{(1)}}{p^{(2)}} = \frac{L_j(T_j^{(1)}) - L_j(T_b)}{L_j(T_j^{(2)}) - L_j(T_b)} \quad \begin{cases} j=3,4 \\ p^{(1)} \neq p^{(2)} \neq 0 \,. \end{cases} \tag{6}$$

Similarly, if eq. (4) is solved for $(1-p)$ instead of p, we arrive at

$$\frac{1-p^{(1)}}{1-p^{(2)}} = \frac{L_j(T_j^{(1)}) - L_j(T_t)}{L_j(T_j^{(2)}) - L_j(T_t)} \quad \begin{cases} j=3,4 \\ p^{(1)} \neq p^{(2)} \neq 1 \,. \end{cases} \tag{7}$$

Although the values of the ratios in eqs. (6) and (7) are unknown, Smith and Rao (1972) have pointed out that they are independent of wavelength and therefore must be the same for all values of j. Hence

$$\frac{L_3(T_3^{(1)}) - L_3(T_x)}{L_3(T_3^{(2)}) - L_3(T_x)} - \frac{L_4(T_4^{(1)}) - L_4(T_x)}{L_4(T_4^{(2)}) - L_4(T_x)} = 0 \quad \begin{cases} T_3^{(1)} \neq T_3^{(2)} \\ T_4^{(1)} \neq T_4^{(2)} \,. \end{cases} \tag{8}$$

In eq. (8) the variable T_x designates some unknown temperature. Examination of the equation (see figure 5) indicates that it has two roots, T_b and T_t, and two discontinuities, $T_3^{(2)}$ and $T_4^{(2)}$. It is possible to solve (8) by an iterative method for T_b and T_t, but the method and the starting guesses must be chosen carefully. My recommendation is to use Brent's (1973a, ch. 4) algorithm. It requires two initial guesses which span the solution, but problems with the discontinuities can be avoided by ensuring that the guesses do not span either discontinuity.

Once T_b is found, it can be used in (5) to find p.

7. Corrections for Atmospheric Effects

Because some of the thermal radiation emitted by the Earth's surface is absorbed and re-emitted by the atmosphere, a radiant temperature measured from space is lower than the true surface radiant temperature. Dual thermal channels, in different wavelength bands, can be used to correct for atmospheric attenuation and thereby determine the absolute surface temperature, to within about 1 K. Prabhakara *et al.* (1974) and Morcrette and Irbe (1978) have shown theoretically that a linear correction of the following form gives the actual surface radiant temperature for a variety of possible atmospheric temperature and water vapor profiles:

$$T_{surf} - T_j = a\,(T_j - T_k) + b \tag{9}$$

T_j and T_k are satellite radiant temperature measurements in two separate channels. The coefficients a and b depend on the wavelength values of the channels. McClain and Abel (1977) have verified the method using coincident satellite and ship data sets. For channels 3 and 4 of NOAA-6 McClain (1980), using the atmospheric radiance model of Weinreb and Hill (1980), has calculated the coefficients to be $a = 0.42$ and $b = 1.3$, when $j = 3$ and $k = 4$.

To determine the necessary atmospheric correction when T_b is known, one need only determine the magnitude of the correction from the pixels surrounding the one containing the target temperature field. From these the additive correction to T_3 and T_4 can be made, and the analysis can proceed as described in section 5.

The case where T_b and p are unknown is somewhat more complicated, but can be solved if there are three, instead of two, pixels where T_b and T_t are the same, but $p^{(1)} \neq p^{(2)} \neq p^{(3)} \neq 0$. Let us introduce the notation $T_{b,3}$ to designate the brightness temperature that the satellite would register if the entire pixel were of the background temperature, i.e., $p = 0$. Let $T_{t,3}$ designate the brightness temperature if the entire pixel were of the target temperature, i.e., $p = 1$. $T_{b,4}$ and $T_{t,4}$ are similarly defined. If we form the ratio $(1-p^{(1)})/(1-p^{(2)})$ we can derive an equation identical to (8) but with two unknowns, $T_{x,3}$ and $T_{x,4}$, instead of one. To solve for these we need an additional equation, which we form from the ratio $(1-p^{(3)})/(1-p^{(2)})$, and thereby convert eq. (8) into two simultaneous nonlinear equations.

$$\frac{L_3(T_3{}^{(k)}) - L_3(T_{x,3})}{L_3(T_3{}^{(2)}) - L_3(T_{x,3})} - \frac{L_4(T_4{}^{(k)}) - L_4(T_{x,4})}{L_4(T_4{}^{(2)}) - L_4(T_{x,4})} = 0 \quad \left\{ \begin{array}{l} k=1,3 \\ T_3{}^{(1)} \neq T_3{}^{(2)} \neq T_3{}^{(3)} \\ T_4{}^{(1)} \neq T_4{}^{(2)} \neq T_4{}^{(3)} \end{array} \right. . \qquad (10)$$

In eq. (10) the variables $T_{x,3}$ and $T_{x,4}$ designate the roots. There are two sets of solutions, $[T_{b,3}, T_{b,4}]$ and $[T_{t,3}, T_{t,4}]$. Once these are determined, T_b and T_t can be found from eq. (9).

8. Discussion

Under some circumstances this algorithm makes possible the determination of temperature fields of subpixel resolution. Potential applications include the following:

[1] It might be possible to determine temperatures of urban heat sources. Tests are being conducted within NOAA to estimate stack temperatures of steel plants using NOAA-6 satellite data with 1.1-km resolution.

[2] The technique might be useful in estimating surface temperatures and areal extents of geothermal areas.

[3] In areas that are partly snow covered, the method could be used to estimate the areal extent of snow in each pixel.

[4] Where there are no cloud-free pixels, but some pixels are not totally cloud-covered, the method still provides a measurement of sea-surface-temperature, including corrections for atmospheric attenuation due to water vapor.

Acknowledgements

This work was initiated and completed while I was supported by a Senior Postdoctoral Research Associateship from the National Research Council, National Academy of Sciences. I am indebted to my colleagues Michael Matson, E. Paul McClain, P. Krishna Rao, Richard Legeckis, Donald R. Wiesnet, and Larry Breaker for comments.

References

Box, M.J., (1966) A comparison of several current optimization problems, and the use of transformations in constrained problems, *Computer Journal,* 9: 67-77.

Brent, R.P., (1973a) *Algorithms for Minimization without Derivatives,* Prentice-Hall, Englewood Cliffs, NJ, 195 pp.

Brent, R.P., (1973b) Some efficient algorithms for solving systems of nonlinear equations, *SIAM Journal of Numerical Analysis,* 10: 327-344.

Forsythe, G.E., Malcolm, M.A., and Moler, C.B., (1977) *Computer Methods for Mathematical Computations,* Prentice-Hall, Englewood Cliffs, NJ, 259 pp.

Kidwell, K.B., (1979) NOAA polar orbiter data (TIROS-N and NOAA-6) users guide, NOAA Satellite Data Services Division, Washington, DC

McClain, E.P., (1980) Multiple atmospheric-window techniques for satellite-derived sea surface temperatures, *COSPAR/SCOR/IUCRM Symposium, Oceanography from Space,* Venice, Italy, May 26-30.

McClain, E.P., and Abel, P.G., (1977) Remote sensing of ocean temperature, *Conference on Satellite Applications to Marine Operations,* New Orleans, LA, November 15-17, 1977, pp. 1-9.

Morcrette, J-J., and Irbe, G.J., (1978) Atmospheric correction of remote measurements of Great Lakes surface temperature, *Proceedings, Fifth Canadian Symposium on Remote Sensing,* Victoria, B.C., August 28-31, 1978, pp. 579-586.

Moré, J.J., and Cosnard, M.Y., (1979) Numerical solution of nonlinear equations, *ACM Transactions on Mathematical Software,* 5: 64-85.

Prabhakara, C., Dalu, G., and Kunde, V.G., (1974) Estimation of sea surface temperature from remote sensing in the 11- to 13-μm window region, *Journal of Geophysical Research,* 79: 5039-5044.

Schwalb, A., (1979) The TIROS-N/NOAA A-G satellite series, NOAA Technical Memorandum NESS 95, Washington, DC, 75 pp.

Smith, W.L., and Rao, P.K., (1972) The determination of surface temperature from satellite "window" radiation measurements, *Fifth Symposium on Temperature,* Washington, DC, June 21-24, 1971, Instrument Society of America, Pittsburgh, PA, pp. 2251-2257.

Suits, G.H., (1975) The nature of electromagnetic radiation, in *Manual of Remote Sensing,* Reeves, R.G., ed., American Society of Photogrammetry, Falls Church, VA, I: 51-73.

Weinreb, M.P., and Hill, M.L., (1980) Calculation of atmospheric radiances and brightness temperatures in infrared window channels of satellite radiometers, NOAA Technical Report NESS 80, Washington, DC, 40 pp.

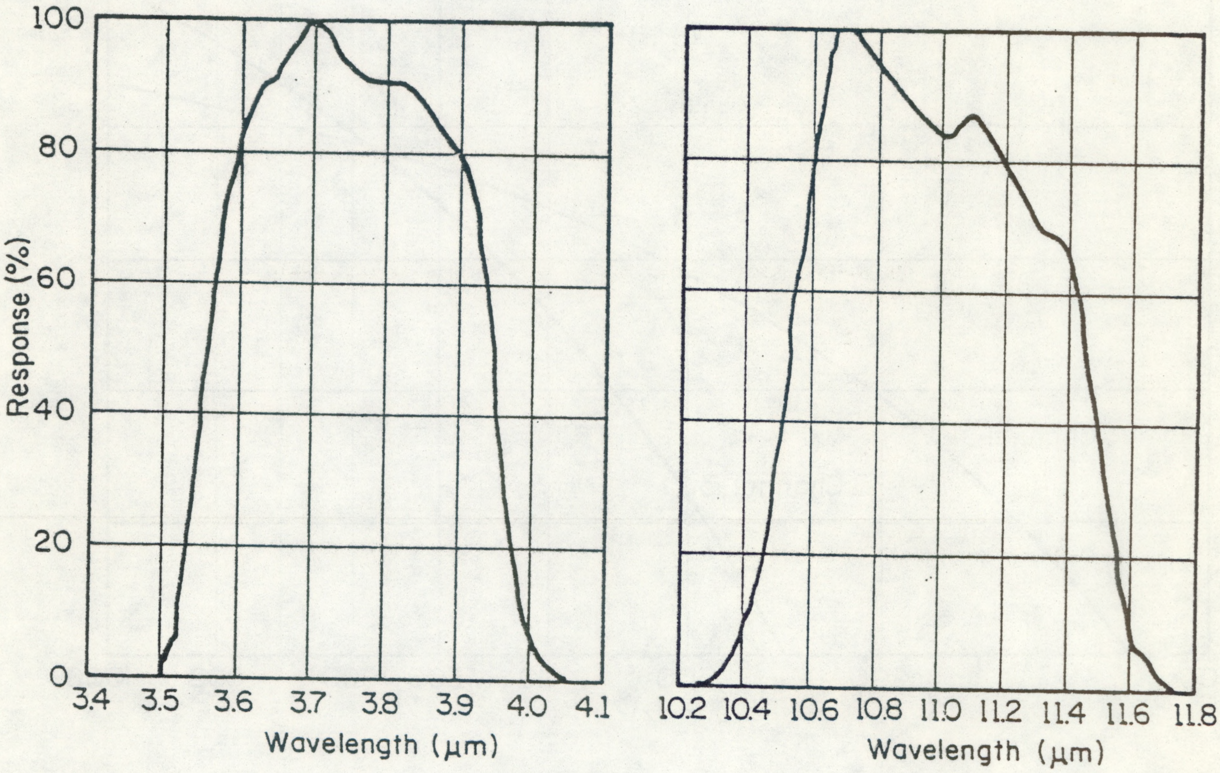

1. Relative spectral response functions (per cent) for channels 3 (left) and 4 (right) of the NOAA-6 satellite (from Kidwell, 1979).

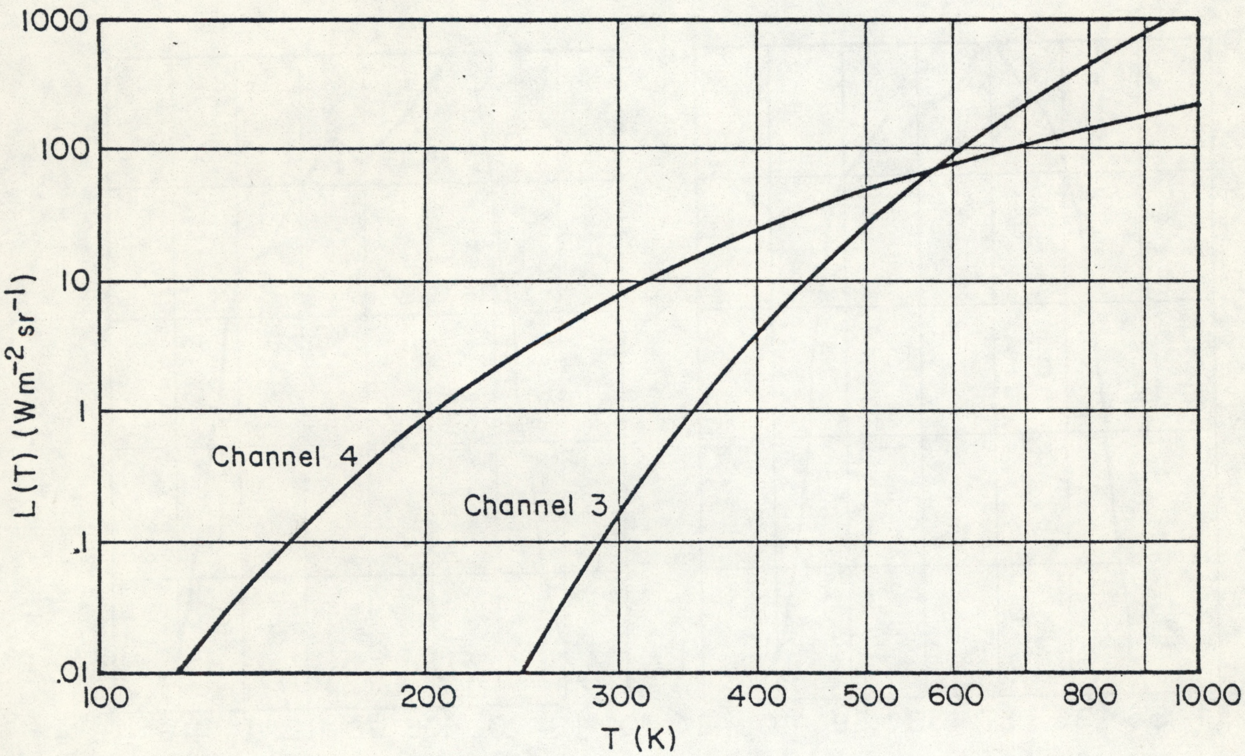

2. NOAA-6 radiances for channels 3 and 4 *vs.* temperature, as calculated by eq. (1) with the spectral response functions in figure 1.

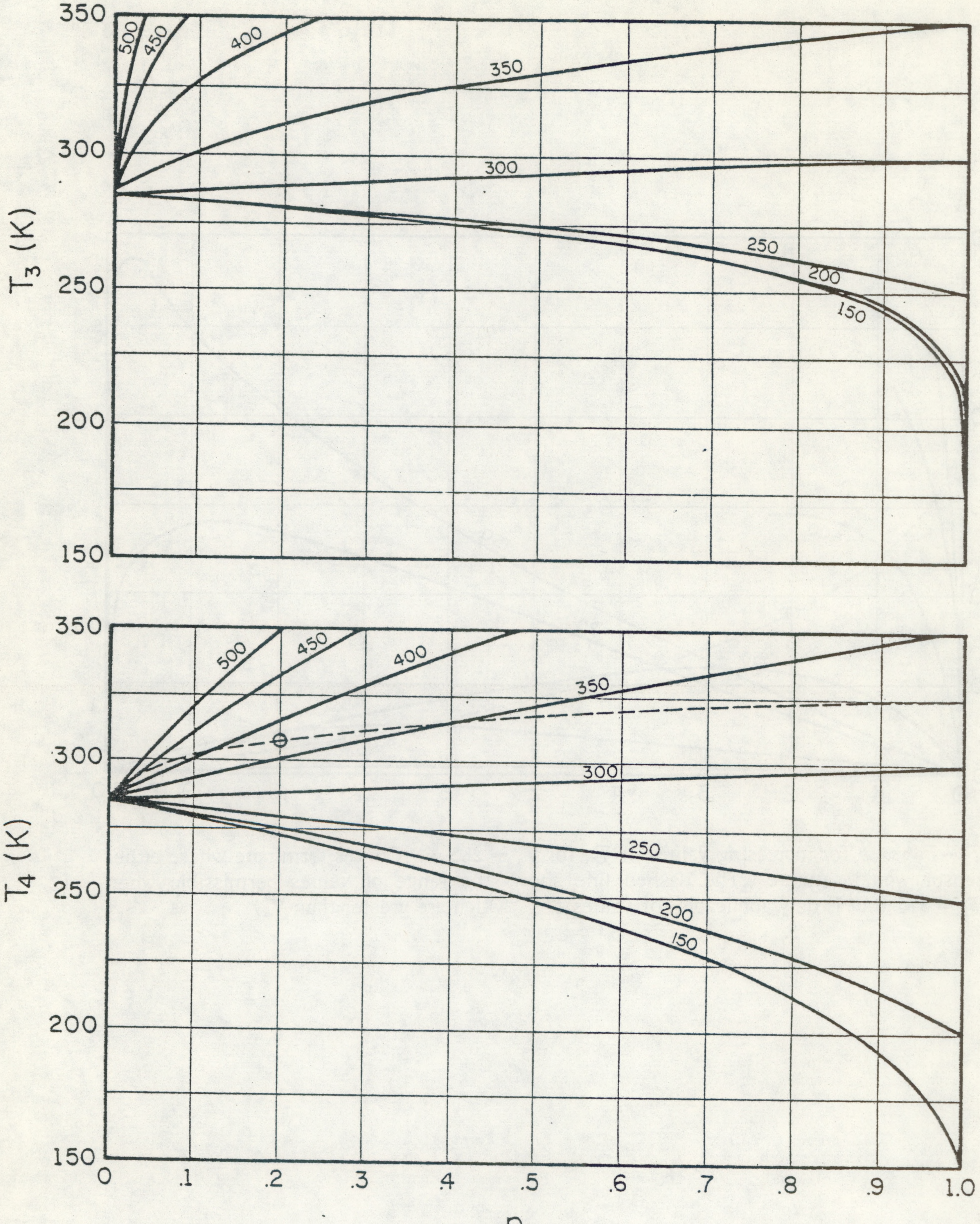

3. T_3 (top) and T_4 (bottom) *vs.* p for increasing values of T_r, for T_b = 285 K. The dashed line in the lower graph shows the range of values permissible when T_3 = 325.

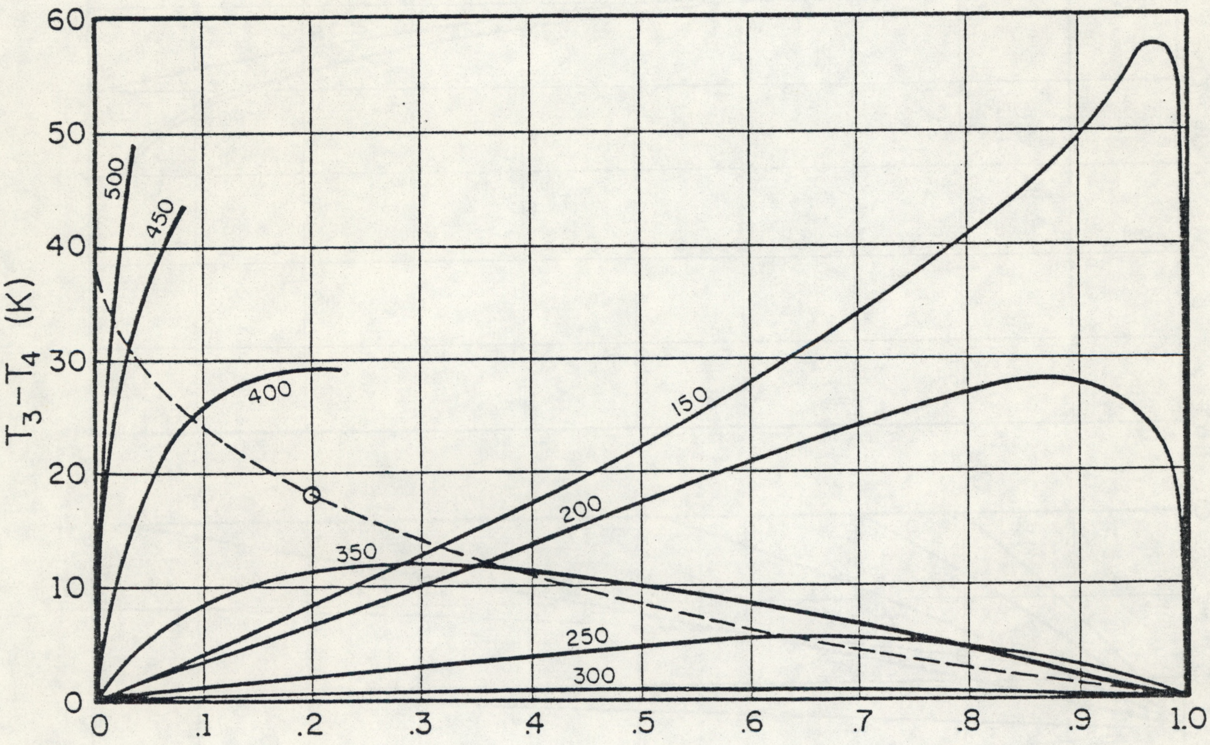

4. $T_3 - T_4$ *vs.* p for increasing values of T_t, for $T_b = 285$ K. Curves terminate where either sensor would saturate. The dashed line shows the range of values permissible when $T_3 = 325$ (but is only applicable for values of T_t which are greater than T_b).

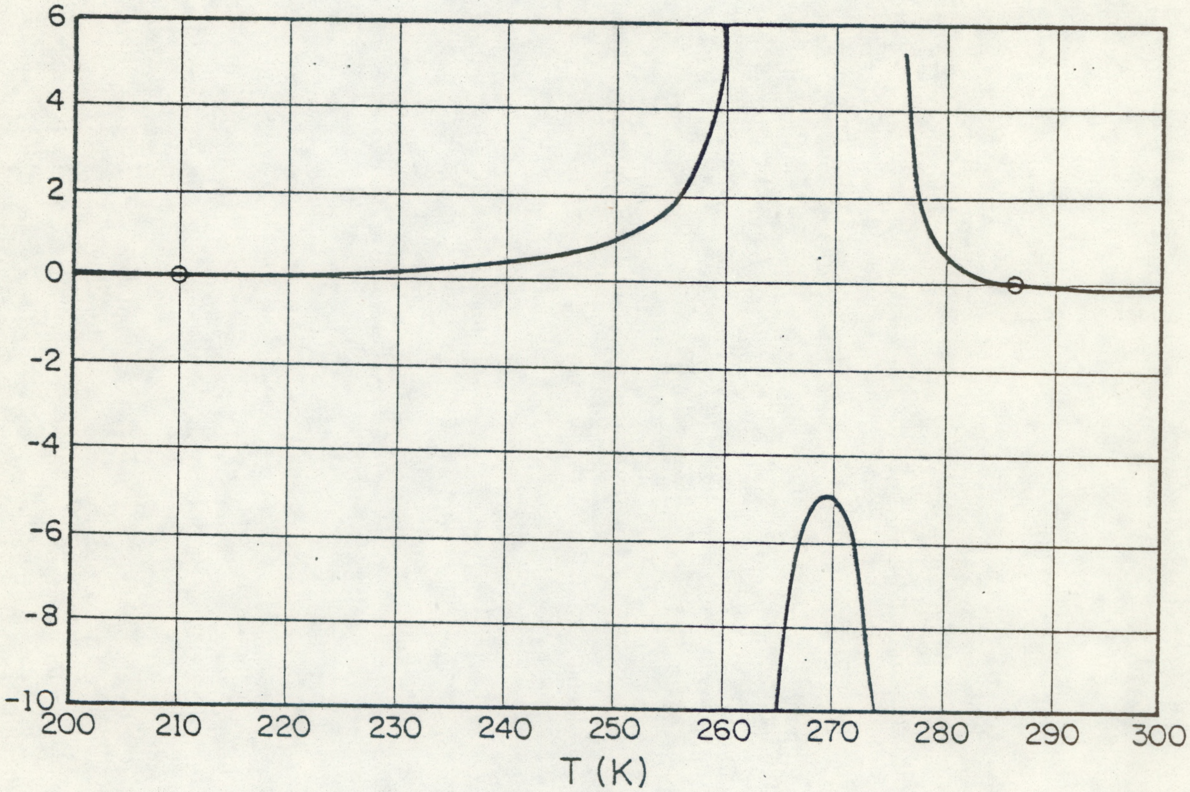

5. Graph of eq. (8) for $T_3^{(1)} = 261.4$, $T_3^{(2)} = 274.6$, $T_4^{(1)} = 241.5$, and $T_4^{(2)} = 262.9$. The solutions are $T_b = 210$ and $T_t = 285$.

(Continued from inside front cover)

NESS 87 Atlantic Tropical and Subtropical Cyclone Classifications for 1976. D. C. Gaby, J. B. Lushine, B. M. Mayfield, S. C. Pearce, K.O. Poteat, and F. E. Torres, April 1977, 13 pp. (PB-269-674/AS)

NESS 88 National Environmental Satellite Service Catalog of Products. Dennis C. Dismachek (Editor), June 1977, 102 pp. (PB-271-315/AS)

NESS 89 A Laser Method of Observing Surface Pressure and Pressure-Altitude and Temperature Profiles of the Troposphere From Satellites. William L. Smith and C. M. R. Platt, July 1977, 38 pp. (PB-272-660/AS)

NESS 90 Lake Erie Ice: Winter 1975-76. Jenifer H. Wartha, August 1977, 68 pp. (PB-276-386/AS)

NESS 91 In-Orbit Storage of NOAA-NESS Standby Satellites. Bruce Sharts and Chris Dunker, September 1977, 3 pp. (PB-283-078/AS)

NESS 92 Publications and Final Reports on Contracts and Grants, 1976. Catherine M. Frain (Compiler), August 1977, 11 pp. (PB-273-169/AS)

NESS 93 Computations of Solar Insolation at Boulder, Colorado. Joseph H. Pope, September 1977, 13 pp. (PB-273-679/AS)

NESS 94 A Report on the Chesapeake Bay Region Nowcasting Experiment. Roderick A. Scofield and Carl E. Weiss, December 1977, 52 pp. (PB-277-102/AS)

NESS 95 The TIROS-N/NOAA A-G Satellite Series. Arthur Schwalb, March 1978, 75 pp. (PB-283-859/AS)

NESS 96 Satellite Data Set for Solar Incoming Radiation Studies. J. Dan Tarpley, Stanley R. Schneider, J. Emmett Bragg, and Marshall P. Waters, III, May 1978, 36 pp. (PB-284-740/AS)

NESS 97 Publications and Final Reports on Contracts and Grants, 1977. Catherine M. Frain (Compiler), August 1978, 13 pp. (PB-287-855/AS)

NESS 98 Quantitative Measurements of Sea Surface Temperature at Several Locations Using the NOAA-3 Very High Resolution Radiometer. Laurence Breaker, Jack Klein, and Michael Pitts, September 1978, 28 pp. (PB-288-488/AS)

NESS 99 An Empirical Model for Atmospheric Transmittance Functions and Its Application to the NIMBUS-6 HIRS Experiment. P.G. Abel and W.L. Smith, NESS, and A. Arking, NASA, September 1978, 29 pp. (PB-288-487/AS)

NESS 100 Characteristics and Environmental Properties of Satellite-Observed Cloud Rows. Samuel K. Beckman (in consultation).

NESS 101 A Comparison of Satellite Observed Middle Cloud Motion With GATE Rawinsonde Data. Leroy D. Herman, January 1979, 13 pp. (PB-292-341/AS)

NESS 102 Computer Tracking of Temperature-Selected Cloud Patterns. Lester F. Hubert, January 1979, 15 pp. (PB-292-159/AS)

NESS 103 Objective Use of Satellite Data To Forecast Changes in Intensity of Tropical Disturbances. Carl O. Erickson, April 1979, 44 pp. (PB-298-915)

NESS 104 Publications and Final Reports on Contracts and Grants. Catherine M. Frain, (Compiler), September 1979. (PB80 122385)

NESS 105 Optical Measurements of Crude Oil Samples Under Simulated Conditions. Warren A. Hovis and John S. Knoll, October 1979, 20 pp. (PB80 120603)

NESS 106 An Improved Model for the Calculation of Longwave Flux at 11 μm. P. G. Abel and A. Gruber, October 1979, 24 pp. (PB80 119431)

NESS 107 Data Extraction and Calibration of TIROS-N/NOAA Radiometers. Levin Lauritson, Gary J. Nelson, and Frank W. Porto, November 1979. (PB80 150824)

NESS 108 Publications and Final Reports on Contracts and Grants. Catherine M. Frain, (Compiler), August 1980.

NESS 109 Catalog of Products, Third Edition. Dennis C. Dismachek, Arthur L. Booth, and John A. Leese, April 1980, 130 pp. (PB81 106270)

NESS 110 GOES Data Collection Program. Merle Nelson, August 1980.

NESS 111 Earth Locating Image Data of Spin-Stabilized Geosynchronous Satellites. Larry N. Hambrick and Dennis R. Phillips, August 1980.

NESS 112 Satellite Observations of Great Lakes Ice: Winter 1978-79. Jenifer Wartha-Clark, September 1980.

NOAA SCIENTIFIC AND TECHNICAL PUBLICATIONS

The National Oceanic and Atmospheric Administration was established as part of the Depart Commerce on October 3, 1970. The mission responsibilities of NOAA are to assess the socioeconomi of natural and technological changes in the environment and to monitor and predict the state of the soli the oceans and their living resources, the atmosphere, and the space environment of the Earth.

The major components of NOAA regularly produce various types of scientific and technical tion in the following kinds of publications:

PROFESSIONAL PAPERS — Important definitive research results, major techniques, and special investigations.

CONTRACT AND GRANT REPORTS — Reports prepared by contractors or grantees under NOAA sponsorship.

ATLAS — Presentation of analyzed data generally in the form of maps showing distribution of rainfall, chemical and physical conditions of oceans and atmosphere, distribution of fishes and marine mammals, ionospheric conditions, etc.

TECHNICAL SERVICE PUBLICATIONS — Reports containing data, observations, instructions, etc. A partial listing includes data serials; prediction and outlook periodicals; technical manuals, training papers, planning reports, and information serials; and miscellaneous technical publications.

TECHNICAL REPORTS — Journal quality with extensive details, mathematical developments, or data listings.

TECHNICAL MEMORANDUMS — Reports of preliminary, partial, or negative research or technology results, interim instructions, and the like.

Information on availability of NOAA publications can be obtained from:

ENVIRONMENTAL SCIENCE INFORMATION CENTER (D822)
ENVIRONMENTAL DATA AND INFORMATION SERVICE
NATIONAL OCEANIC AND ATMOSPHERIC ADMINISTRATION
U.S. DEPARTMENT OF COMMERCE

6009 Executive Boulevard
Rockville, MD 20852

NOAA--S/T 80-312